Estimation of Microblock Sizes in Mosaic Crystals according to Fast Electron Radiation Characteristics

D. A. Baklanov, I. E. Vnukov, S. A. Laktionova, and R. A. Shatokhin

Belgorod State University, Belgorod, Russia

Received January 11, 2012

Abstract—The possibilities of a previously proposed technique for determining the characteristic sizes of microblocks in mosaic $a\alpha$-class crystals have been analyzed. Determination is performed according to the ratio between the measured and calculated values for the diffraction suppression of the fixed-energy bremsstrahlung yield. The limits of applicability of the technique have been revealed. It is demonstrated that the technique can be implemented in an electron accelerator with the average energy $E_e \sim 30$–40 MeV and long baselines making it possible to use crystal-diffraction spectrometers. The influence of microblock sizes on coherent electromagnetic processes in real crystals is discussed.

INTRODUCTION

The ordered arrangement of atoms of a condensed material leads to the orientational and interferential effects observed in the yield of secondary processes, which arise from the penetration of fast electrons into the material. The interdependence between a target's structure and the yield of secondary processes enables us to analyze the target's structure on the basis of measurement data. For example, the locations of impurities in a crystal lattice can be estimated according to the yield of backscattered channeled ions, and the potential shape, electron density, the amplitude of thermal oscillations of lattice atoms, and so forth can be defined more exactly during fast electron channeling [1, 2].

In this series is also the problem concerning the qualitative and structural analysis of crystal samples, i.e., the determination of extrinsic impurities, mosaic blocks, and the distributions of microblocks over the angle of disorientation with respect to the main direction and over sizes and the characteristics of hard electromagnetic radiation generated by the passage of fast electrons. This approach is advantageous due to the high penetration capability of radiation and visualization of interpretation. These properties are most distinctly implemented in analyzing the microstructure of thick samples and solving the problem of estimating the characteristic sizes of blocks, where X-ray diffraction analysis cannot ensure quality control of the structure.

From the standpoint of the degree of perfection, crystals are known to be classified by two criteria: the size of regular blocks (or regions) and the degree of mutual disorientation of the blocks [3]. The first criterion enables us to divide all crystals into a and b classes. In a-class crystals, blocks are large enough to manifest the conspicuous effect of primary extinction; i.e., their linear sizes are commensurable with primary extinction length l_{ex}. b-class crystals contain only regular blocks of small size. Hence, the effect of primary extinction is hardly observable. According to the second criterion, crystals can be divided into α and β classes. α-class crystals have almost parallel blocks, and their mutual disorientation is small. As a result, the contribution of secondary extinction is insignificant. In β-class crystals, the distribution of blocks is irregular, leading to the low contribution of secondary extinction. When the disorientation of microblocks is smaller than the X-ray total reflection region $\Delta\Theta$ (the Darwin table width), the limits of $a\alpha$ and $b\beta$ classes are perfect and ideal mosaic crystals, respectively.

As is evident from the foregoing, the most complicated problem is determination of the characteristic sizes of blocks, which often affects the possibility of the practical usage of crystals. To extract beams from high-energy accelerators [4], perfect crystals, or at least $a\alpha$-class ones, are necessary. In medicine [5], X-ray and gamma-ray astronomy [6], and the creation of intense quasi-monochromatic neutron beams [7], mosaic crystals of $b\alpha$ class are required. It should be emphasized that one or another class of crystals is not once and for all specified due to its coupling with the quantity l_{ex}, determined by the order of reflection and the photon energy [3]. In other words, the same sample can belong to different classes, depending on the reflection order or the photon energy [8].

The direct measurement of microblock sizes with the help of X-ray beams is a complex experimental problem and can be implemented only in analysis of surface layers [9]. This problem can be solved via electron microscopy as applied to thin polycrystalline and

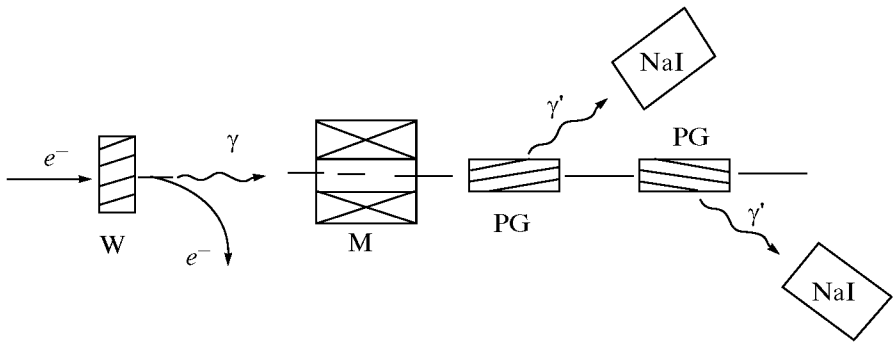

Fig. 1. Experimental equipment scheme [12]: W is the tungsten crystal, M is the purifying magnet, PG is the pyrolytic graphite crystal, and NaI is the NaI(Tl) spectrometer.

crystalline samples if the disorientation angles of neighboring blocks and their sizes exceed the divergence and linear sizes of the electron beam on the target [10]. If thin crystalline targets (for example, metallic crystals) cannot be produced without structural violations, electron microscopy will not provide the necessary information.

When fast electrons are employed instead of X-rays with a fixed wavelength or electron microscopy methods, more qualitative data on the microstructure of thick crystals can be obtained by varying the observation angle [8] and the photon energy recorded [11], in particular, it is possible to estimate the characteristic sizes of microblocks. Hence, estimating the quality of the crystal structure, as well as determining the characteristic sizes of microblocks via radiation generated by fast electrons passing through them, are important and topical problems.

EXPERIMENTAL EQUIPMENT AND MEASUREMENT TECHNIQUE

Our technique for estimating the characteristic sizes of microblocks in $a\alpha$-class crystals is based on experimental results [12], in which parametric X-ray radiation (PXR) was sought and investigated at small angles to the particle velocity in a tungsten crystal. The scheme of the experiment is shown in Fig. 1. Electrons accelerated up to the final energy $E_0 = 500$ MeV hit a monocrystalline target mounted in a goniometer. The radiation under study passed through a collimator, was purified by a magnet, and came into an experimental hall with recording equipment. The experimental equipment's characteristics and the data measurement and processing technique are reported in [11–13].

Measurements were performed using a cylindrical tungsten monocrystal ∅8.5 mm in diameter and 0.41 mm^3 long with the $\langle 111 \rangle$ orientation and the surface mosaicity $\sigma_m \leq 0.2$ mrad. The crystal was arranged in the goniometer so that its (112) plane was rotated relative to the vertical plane at the angle $\beta = 3.5° \pm 0.2°$. Such an arrangement made it possible to investigate the orientation effects created by the $(11\bar{2})$ plane and two (110)-type planes rotated around it by 30°.

Two crystal-diffraction spectrometers based on mosaic pyrolytic graphite (PG) crystals with dimensions of 2.5 × 6.5 × 22.5 and 3.5 × 5.5 × 20 mm were used to extract the fixed-energy radiation. The crystals were mounted in goniometers at distances of 13–15 m from the tungsten crystal generating the radiation under study. The diffracted radiation was recorded by NaI(Tl) detectors, each 40 mm in diameter and 1 mm^3 long. The distance between the detectors and the graphite crystals was 3–5 m. The mosaicity distributions of the graphite crystals were determined by measuring the diffraction curve and identifying the diffraction peak at each angle of the detector's position used in the experiment [13].

The energy resolution of spectrometers depends weakly on the crystal mosaicity under the conditions mentioned above, and its values are determined by the angular apertures of the spectrometers and the collimation angle of the diffracted radiation. In the diffraction (horizontal) plane, the radiation collimation angle $\Delta\Theta_x = 0.4$–0.7 mrad. Hence, the spectrometer resolution $\Delta\omega/\omega \sim 0.5$–$2\%$, depending on the input energy of the diffractometers. Since NaI(Tl) crystals 1 mm thick and differential discriminators were chosen as detectors, only the first allowable order of reflection was determined, the background was substantially decreased, and the attained peak/substrate ratio of a diffraction curve was about 20–70, depending on the photon energy recorded. In other words, the contribution of background photons with energies differing from the fixed value did not exceed 1.5–5%.

From the viewpoint of the posed problem, the most important experimental result [12] was the discovery of diffraction suppression of the bremsstrahlung yield, i.e., minima in the orientation dependences (ODs) of the yield of high-energy photons with $\omega \approx \gamma\omega_p$. Here, γ is the Lorentz coefficient and ω_p is the plasma frequency of a medium (Fig. 2). The positions of the minima corresponded to the kinematic conditions of

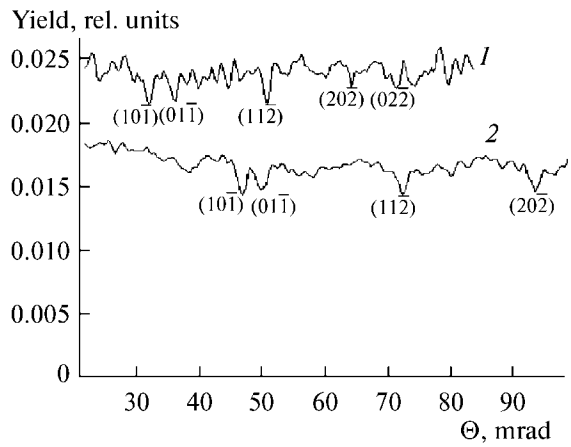

Fig. 2. ODs of the X-ray yield from the tungsten crystal in the experiment [12]: ω = (*1*) 96 and (*2*) 67 keV.

diffraction of the aforementioned photons with an error of less than 1%. The depth of the minima varied from ~15 (ω = 67 keV) to ~10% (ω > 90 keV). The full width of the minima was about 1.5–2.5 mrad.

With allowance for the spectrometer's efficiency and the contribution of transient radiation from the output face of the crystal, the ODs of the X-ray yield have been calculated in [11] under experimental conditions [12]. The calculations were carried out with the help of an approximate technique for evaluating bremsstrahlung diffraction in perfect crystals [14]. The evaluated data have demonstrated that the positions of the minima that appeared agree well with calculations involving weak reflections of the (112) and (220) planes. However, for the (110)-type planes and photon energies of 67 and 96 keV, the dip depths of the calculated ODs turned out to be ~2.5 and ~1.5%, respectively. Thus, they were less than the experimental dips (~15 and ~10%, respectively) by a factor of about 5. The widths of the calculated curves were less than those of the experimental curves by a factor of approximately 1.5–2. In comparison of the calculated and measured results, the spectral distributions of the efficiency of the crystal-diffraction spectrometers, which were obtained using the specially developed technique for evaluating the spectrometer efficiency on the basis of mosaic *b*-class crystals with the help of statistical simulation [15], were used.

Relying on the results discussed above and proceeding from the fact that the dynamic effect in the radiation of fast electrons, which by default confirms the structure's perfection—PXR along the particle velocity, i.e., the so-called forward PXR—was observed for the first time in the experiment [12], the authors of [11] attributed the used tungsten crystal to the $a\alpha$ class and proposed estimation of the sizes of perfect blocks in such crystals via two methods: according to the degree of FPXR at photon energies $\omega < \gamma\omega_p$ and bremsstrahlung diffraction at energies $\omega > \gamma\omega_p$ (i.e., the ratio between the experimentally determined diffraction suppression of the fixed-energy photon yield in a mosaic crystal and calculations or measured results obtained for a perfect crystal). In implementation of the first method, it is necessary to employ an accelerator with an energy of about 1 GeV, which is economically unjustified. Hence, the second method is of interest and can find application because such measurement can be performed by means of lower-energy accelerators.

ESTIMATION OF BLOCK SIZES FROM DIFFRACTION SUPPRESSION OF THE BREMSSTRAHLUNG YIELD

In mosaic crystals, the characteristic sizes of microblocks are estimated via the technique based on diffraction suppression of the bremsstrahlung yield [11] and two assumptions. The first is that the crystal under study is a mosaic $a\alpha$-class crystal. In other words, typical microblock sizes are substantially greater than the primary extinction length l_{ex} for the given reflection order and photon energy ω. The second implies the negligibly small probability that a diffracted photon will be repeatedly reflected in other microblocks.

In the case of the crystal used in the experiment [12], the first assumption is valid because the first time that forward PXR was detected was implemented under the corresponding condition. The dip arising in the high-energy photon yield, the depth of which noticeably exceeds the contribution of diffraction suppression of the high-energy photon yield in perfect crystals, is unambiguous evidence of mosaic structure along the photon beam direction because there is no other reason for the level of suppression observed in the experiment. Other evidence is the dip width which appreciably exceeds the value predicted by calculations for a perfect crystal. In the case of any other crystal, fulfillment of the assumption must undoubtedly be checked.

The surface mosaicity of the tungsten crystal used in the experiment [12] was $\sigma_m \leq 0.2$ mrad. However, this value actually corresponds to the sensitivity of the procedure of certification of crystal surfaces. Thus, the true volume mosaicity can be either less or greater than this value and is comparable with the total reflection region $\Delta\Theta \sim 0.03$ mrad. Hence, for determination of the limits of the applicability of technique [11], supplementary investigations into the influence of repeated reflections on the determined extent of suppression are necessary.

To obtain an exact solution to the problem concerning the contribution of repeated reflections, the unknown microblock distributions over the angles of disorientation and over sizes are necessary, which, strictly speaking, must be revealed from measurement results. Hence, we will analyze how these parameters affect the measured fixed-energy photon yields when

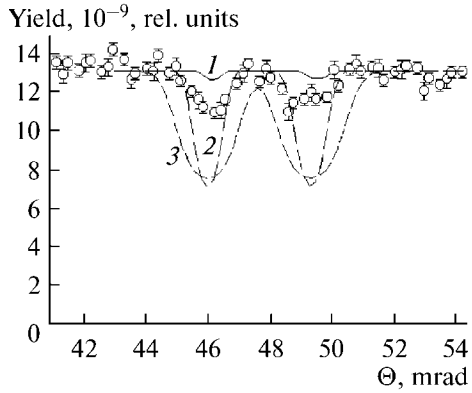

Fig. 3. OD of the yield of photons with $\omega = 67$ keV. Dots designate the experimental data [12]. Curves *1–3* are obtained for a perfect crystal and $\sigma_m = 0.2$ and 0.5 mrad, respectively.

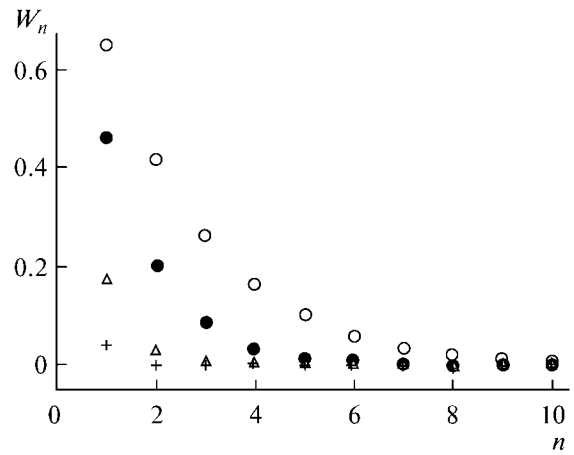

Fig. 4. Dependences of the quantity W_n on the crystal mosaicity. Here, unfilled and filled circles, triangles, and pluses were obtained at $\sigma_m = 0.2$, 0.5, 2, and 10 mrad, respectively.

the crystal of interest belongs to the $b\alpha$ class. Analysis is performed via the simulation technique [15] which is developed for such crystals and rather well describes the measured results. In [11, 16], this approach was employed to calculate the efficiency of crystal-diffraction spectrometers.

The measured OD of the yield of photons with $\omega =$ 67 keV and three ODs calculated for tungsten crystals 0.41 mm thick with perfect and two mosaic microstructures are compared in Fig. 3. The perfect crystal yields were determined by means of the technique reported in [14]. The data on the mosaic crystals with $\sigma_m = 0.2$ and 0.5 mrad were calculated via the technique described in [15], i.e., under the assumptions that the characteristic sizes of the microblocks of a mosaic crystal are smaller than the primary extinction length of photons with this energy ($l_{ex} \approx 3.1$ μm) and the number of blocks within the absorption length $l_a \approx$ 183 μm exceeds 50–100 (dependences *1–3*). The calculations were performed with allowance for the efficiency and angular capture of the crystal-diffraction spectrometer. The measured results were normalized to the calculated data in the region without the influence of diffraction effects. The experimental errors are statistical and do not contain errors of normalization and determination of the NaI(Tl) detector used in the cited work.

It is seen in Fig. 3 that the mosaic crystals have wider dips than the perfect crystal and their depths are considerably larger. As might be expected, none of the dependences coincides with the measured results because the tungsten crystal used in the experiment [12] has the $a\alpha$ class instead of $b\alpha$. However, its estimated volume mosaicity is close to $\sigma_m \approx 0.2$ mrad because curve *2* with $\sigma_m = 0.2$ mrad exhibits better agreement with the experimental dependence than curve *3* with $\sigma_m = 0.5$ mrad.

As is clear from Fig. 3, diffraction suppression hardly depends on changes in the quantity σ_m and is about 45% in both cases. For mosaic *b*-class crystals, the X-ray reflectance $Q \sim z^2$, and the reflection probability $W \sim Q/\sigma_m^2$ [15]. Hence, for small values of σ_m, the re-reflection probability abruptly increases. To confirm the aforesaid, the calculated quantity W_n, i.e., the probability that a photon undergoes no less than *n* reflections before its absorption in or escape from a crystal (the value averaged over the energy capture of the spectrometer), is presented in Fig. 4. The value of *n* varies from unity to 17–18, depending on the mosaicity σ_m. Calculations were performed under the conditions of the experiment [12] and for four values of σ_m.

It is seen from Fig. 4 that the probability of one or more reflections is greater in the crystal with $\sigma_m =$ 0.2 mrad (~65%) than in the crystal with $\sigma_m =$ 0.5 mrad (~46%) and exceeds the diffraction suppression of the photon yield (~45%). The total suppression of the bremsstrahlung yield is determined by the ratio between odd and even reflections. Odd reflections reduce the recorded yield, while even ones partially compensate for this loss (Fig. 5).

It follows from Fig.5 that, at $\sigma_m = 0.2$ mrad, the percentage of photons that experienced only one reflection corresponding to the observed diffraction suppression (~23%) is significantly smaller than the diffraction suppression (~45%) and is somewhat smaller than the value inherent to the crystal with $\sigma_m =$ 0.5 mrad (~26%). At the same time, the probability of all subsequent reflections in the crystal with a smaller value of σ_m is substantially higher. Thus, for these two crystals, the resultant suppressions of the yield turn out to be closely coincident (Fig. 3, curves *2*, *3*). With increasing characteristic angle of mosaicity, the probability of multiple reflections abruptly decreases. In the case of the photon energy $\omega = 67$ keV, the proba-

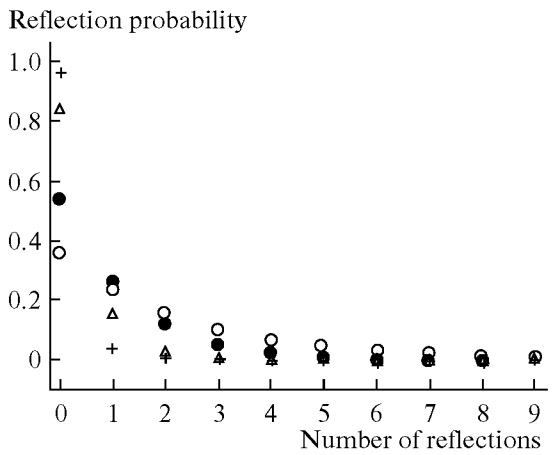

Fig. 5. Dependences of the reflection probability on the crystal mosaicity. Here, unfilled and filled circles, triangles, and pluses were obtained at σ_m = 0.2, 0.5, 2, and 10 mrad, respectively.

bility of repeated reflection is less than the probability of single reflection by a factor of 10. Therefore, at large values of σ_m, the effect of multiple reflections can be disregarded. It should be emphasized that the reflectance of b-class crystals is $Q \sim \lambda^2$. Hence, when the photon energy changes, the limiting σ_m, at which the re-reflection effect can be disregarded, must be determined once again.

The performed analysis indicates the significantly different diffraction suppression of the radiation yield obtained with and without allowance for multiple reflections. For $a\alpha$-class crystals, the situation is much more complicated because data on the size distribution of blocks are not available. In this case, exact statistical analysis is impossible. It is likely that such a problem can be solved via the convergence method with the help of information on the distributions of blocks over disorientation angles and sizes.

If the aforementioned data are not available, the number and characteristic sizes of blocks can be determined by means of a technique based on the diffraction suppression of the photon yield. However, in this case, the determined suppression must be substantially smaller than the suppression corresponding to the $b\alpha$-class crystal with the same value of σ_m. If this condition is not satisfied and they are commensurable, the number of blocks turns out to be underestimated, and, on the contrary, the characteristic size is significantly overestimated. This difficulty can be surmounted with the help of weaker orders of reflection, at which the characteristic angular region of total reflection and, accordingly, the re-reflection probability become appreciably smaller.

For the tungsten crystal used in the experiment [12] and the photon energy ω = 67 keV, this condition is fulfilled. The determined diffraction suppression of the radiation yield (~17%) (Fig. 3) is much smaller than the suppression calculated for the $b\alpha$-class crystal with the same thickness and characteristic angle of mosaicity (~45%). Hence, the ratio between the depths of the experimental and calculated minima in the radiation yield (~5.4) [16] can be chosen as the estimated number of blocks along the photon path in a crystal.

As was noted above, the diffraction suppression inherent to a perfect crystal (Fig. 3, curve *1*) was calculated under the assumption that the diffraction process is not affected by photon absorption [14]. When a monodirectional and monoenergetic photon beam and blocks with a thickness of up to 50 μm are employed, comparison between this approach and the more accurate approach [17] has demonstrated that the difference in the diffraction suppressions calculated via these approaches does not exceed 20%. Hence, it is reasonable to estimate the number of blocks with the help of the simpler technique [14]. At the photon energy $\omega = 67$ keV, $\sigma_m \approx 0.2$ mrad exceeds the characteristic total reflection region $\Delta\Theta \sim 3 \times 10^{-5}$ rad by almost an order of magnitude. Hence, when a photon can hit at least five blocks, the probability of the repeated reflection of a singly diffracted photon can be disregarded in the first approximation.

The formation of the experimentally measured fixed-energy photon yield is related to their decrease due to diffraction or absorption and generation caused by electron passage through the crystal under study. Hence, the effective mean free path of photons in a crystal must be chosen as the characteristic distance corresponding to the formation of the recorded radiation yield, instead of the photon absorption length l_a, as was done in [11]. In other words, it is necessary to use the mean distance covered by the photon that has escaped from a crystal into the spatial angle overlapped by the crystal-diffraction spectrometer:

$$\langle l_{\rm ph}\rangle = \frac{\int_0^T (T-t)dt \int d\omega \int \frac{d^2 I^*}{d\omega d\Omega} S(\omega, \mathbf{n}, t) d\Omega}{\int_0^T dt \int d\omega \int \frac{d^2 I^*}{d\omega d\Omega} S(\omega, \mathbf{n}, t) d\Omega},$$

where $\frac{d^2 I^*}{d\omega d\Omega}$ is the spectral-angular distribution of the bremsstrahlung intensity with allowance for the multiple scattering of electrons in a target [14], $S(\omega, \mathbf{n}, t)$ is the coefficient characterizing the absorption of photons with the direction of motion $\mathbf{n}$ and energy ω in a target material and the efficiency of the crystal-diffraction spectrometer, and T is the crystal thickness. Integration is performed over all escape angles and photon energies with allowance for the angular and energy capture of the spectrometer. According to simulation, the re-reflection-induced changes of the photon-path length in the material hardly affect the quantity $\langle l_{\rm ph}\rangle$ at all. Hence, at the assigned values of ω and T, this quantity can be regarded as invariable.

The effective length depends on both the electron and photon energies and the crystal thickness. When the crystal thickness increases and the electron energy decreases, the quantity $\langle l_{ph} \rangle$ increases due to the stronger influence of the multiple scattering of electrons in the crystal. At the photon energy $\omega = 67$ keV in a tungsten crystal 0.41 mm thick, $\langle l_{ph} \rangle$ 236 μm $> l_a \approx 184$ μm.

The contributions of blocks to the minimum of the measured radiation yield are determined by the distribution of microblocks over the crystal volume and the characteristic angle of mosaicity. At large disorientation angles of a block with respect to the main direction, the energy of photons diffracted by the block is beyond the energy capture of the spectrometer. Therefore, there is no block contribution to the recorded diffraction suppression. If the energy change $\Delta\omega$ of diffracted photons is smaller than the energy capture ΔE of the spectrometer (i.e., $\Delta\omega \sim \omega \frac{\cos\Theta}{\sin\Theta} \Delta\Theta \leq \Delta E$, where $\Delta\Theta$ is the maximum spread in the angular distribution of mosaic blocks with respect to the main direction), this effect can be disregarded. If this condition is not satisfied, the percentage of blocks excluded from the formation of the diffraction suppression of the fixed-energy photon yield must be determined according to the distribution of microblocks over the disorientation angles. In addition, in determination of the characteristic length of a block, the corresponding corrections must be applied.

In the case of the tungsten crystal used in the experiment [12], this condition is sufficiently well fulfilled. Let the disorientation angles of the blocks with $\sigma_m \approx 0.2$ mrad have Gaussian distribution (Fig. 3). In this case, if angle $\pm 2\sigma_m$ containing the disorientation angles of ~95% of all blocks is chosen as $\Delta\Theta$, the estimated quantity $\Delta\omega \approx 1.3$ keV will be close to the energy capture $\Delta E \approx 1.2$ keV [15]. This implies that all blocks located near the effective path length of the recorded photons participate in diffraction suppression. Therefore, in this tungsten crystal, the characteristic sizes of the blocks are $l_{bl} \approx \langle l_{ph} \rangle / N_{bl}$ ~40–45 μm instead of ~30 μm.

In measurements of the characteristic sizes of microblocks in $a\alpha$-class crystals, it is not necessary to use an accelerator with an energy of ~1 GeV as in the experiment [12]. Since the X-ray diffraction process is independent of the electron energy, relatively inexpensive electron accelerators with energies of 30–50 MeV can be employed to perform the measurements. However, the baselines must be sufficiently long to implement the technique of extracting radiation of fixed energy with the help of crystal-diffraction spectrometers. In this case, the functional diagram of the setup intended for the implementation of the proposed technique is similar to the scheme shown in Fig. 1.

The application of electrons with lower energies is beneficial because the X-ray frequency range has no forward PXR capable of masking the diffraction suppression of the radiation yield [11, 12] underlying the analyzed technique of estimating the characteristic sizes of microblocks. Thus, measurements can be carried out at lower photon energies, thereby restricting the crystal region under consideration and the number of blocks contributing to the recorded suppression of the photon yield.

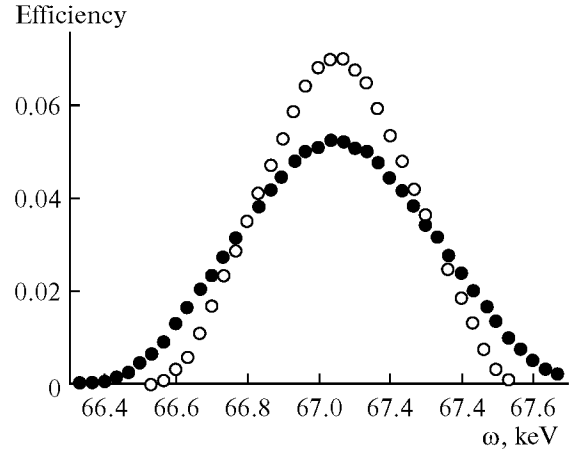

Fig. 6. Efficiency of the crystal-diffraction spectrometer at $E_e = 50$ MeV and $\omega = 67$ keV. Here, unfilled and filled circles designate a point beam and a beam with a size of 5 × 16 mm, respectively.

From the viewpoint of the analyzed technique of estimating the quality of crystal structures and the characteristic sizes of microblocks, an important distinction between high- and moderate-energy accelerators is that the latter ensure a substantially larger electron beam size on a target: 5 × 10 mm or more [18]. The resolution and efficiency of the crystal-diffraction spectrometer depend on the angular distribution of radiation incident on the crystal-analyzer and the distances between the target generating the radiation under study, the crystal-analyzer, and the diffracted radiation detector. A change in the size of the radiating region varies the angular distribution of radiation on the crystal-analyzer and can worsen the recorded radiation monochromaticity and, consequently, the sensitivity of the proposed technique.

To check the influence of changes on the spectrometer resolution according to the technique [15], the efficiency of the crystal-diffraction spectrometer was simulated on the basis of a mosaic PG crystal 2.5 mm wide at different cross sections of an electron beam falling on the crystalline sample of interest. The simulation results obtained at electron and photon energies of 50 MeV and 67 keV, respectively, are depicted in Fig. 6. Other conditions coincide with those of the experiment [12] performed at this photon energy. In the first case (the results are designated by unfilled circles), the size of the electron beam was not taken into account (the point-beam approximation). In the second case (the results are designated by filled circles), the vertical and horizontal sizes of the electron beam were 5 and 16 mm, respectively.

As is seen in Fig. 6, the increased sizes of the electron beam do not affect the characteristics of the spec-

trometer. The area below two dependences (the total efficiency of the spectrometer) varied by less than 2%. However, the resolution reduced by ~30%. Therefore, as can be expected, changes in the depth and wide of the OD minimum, which arise from the diffraction suppression of the bremsstrahlung yield in the perfect crystal, will be approximately identical. In connection with this, it should be noted that, for the conditions of the experiment [12], the ODs of the radiation yield calculated for the same sizes of the electron beam on the tungsten crystal turned out to be absolutely identical.

Another feature of a microtron and a linear accelerator (the most widespread electron accelerators of moderate energy) is the short acceleration cycle: ~6–10 μs. Its duration is comparable with the typical pulse width of the NaI(Tl) detector (~1–8 μs, depending on the type of detector used). Hence, to eliminate superpositions and extract photons with a single reflection order by means of a differential discriminator (as was done in the experiment [12]), the accelerator current must be maintained so that only 0.2–0.4 pulses can be recorded over one cycle of acceleration [19].

To obtain statistical error at level of 1–2% at an accelerator frequency of 50 Hz, the exposure time of each crystal orientation must be no less than 400 s. The reliable extraction of the effect of diffraction suppression can be implemented by measuring the radiation yield at 100–200 points with a step of no more than ~0.1 mrad. As a result, the 15-h continuous operation of an accelerator is required. To adjust the orientation of the crystal-analyzer of the spectrometer and find the diffraction suppression regions for each desired plane of the crystal under study, approximately the same time is required. When the accelerator frequency is reduced to 10 Hz (as was done, e.g., in [20]), the duration of one measurement becomes practically inadmissible.

Such a drawback can be overcome with the help of a diffracted radiation detector in the integral mode. As was demonstrated in [20], this mode of detector operation makes it possible to measure the ODs of the radiation yield at 500 points. Measurements were performed for 30–40 min with an error of ~1–2% even when the detector was located in the experimental hall. If the detector is reliably protected against the background, the contribution of photons not participating in the diffraction process is less than 3–5% [13, 16], confirming the possibility of implementing this measurement scheme.

In the operation mode described above, the radiation from several orders of reflection (instead of one order as in the experiment [12]) is simultaneously recorded and, consequently, can be interpreted only during processing of the measured results. It should be emphasized that the integral reflectance of the PG crystal is less in the second order of reflection than in the first order by a factor of at least 20–25 [13]. Hence, the contribution of high-energy photons to the recorded suppression of the radiation yield will be approximately the same. If necessary, the contribution of the second and successive orders of reflection can be decreased by selecting a detector with a low efficiency at these photon energies. The low-efficient detector also enables us to reduce the contribution of the high-energy background of rescattered bremsstrahlung.

One of the main advantages of the proposed technique for investigating the microstructure of crystalline samples is the possibility of varying the photon energy within wide limits (up to 100–150 keV). As a result, the thickness of the samples under study can be increased and the mutual disorientation of blocks at an angle of $\sim 10^{-5}$ rad can be observed. This effect cannot be revealed by means of photons with $\omega \sim 10$ keV or less because the angular region of total reflection, which restricts the sensitivity of traditional X-ray diffraction methods to the mutual disorientation of blocks inside the crystal, $\Delta\Theta \sim \omega^{-1}$ is $\sim 10^{-4}$ at these photon energies. Another main advantage of the proposed technique is the possibility of estimating the number and characteristic longitudinal sizes of blocks in almost perfect $a\alpha$-class crystals. Note that such information cannot be obtained via other traditional methods [10].

As was ascertained in [11], the limitation of block sizes can suppress the yield of the coherent bremsstrahlung of fast electrons in a mosaic crystal and the related positron yield [21] if the disorientation angle of adjacent blocks exceeds the characteristic radiation angle γ^{-1} and their size is less than the radiation formation length, or the so-called coherent length: $l_{\text{coh}} \approx \delta^{-1}$. Here, $\delta = \frac{1}{2E}\frac{x}{1-x}$ is the minimum transferred longitudinal momentum, where $x = \omega/E$ is the relative photon energy and E is the particle energy. The system of units $\hbar = m_e = c = 1$ is used. The existence of this effect is caused by the suppression of the coherent bremsstrahlung yield at a crystal thickness of $T \leq l_{\text{coh}}$ [22].

Owing to the finiteness of microblock sizes, the effect of suppression of the coherent bremsstrahlung yield can manifest itself only if the formation length is comparable with the microblock sizes of a real crystal, i.e., is no less than several tens of micrometers. Since coherent amplification of the radiation yield is observed if the condition $g_l \approx \delta$ is fulfilled (here, $g_l \approx g\sin\psi$ is the longitudinal momentum transferred to the crystal during radiation, g is the crystal's reciprocal-lattice vector, and ψ is the angular disorientation of the axis or crystal plane with respect to the particle motion direction), to satisfy this condition, the angle of electron incidence with respect to the fundamental crystallographic directions must be small ($\sim 10^{-4}$ rad).

As is known [1], a particle trajectory is bent if the particle incidence onto the axis or plane is at an angle smaller than the critical angle ψ_c of axial or planar channeling. Its capture into the motion mode is possible under the condition of axial or planar channeling. The periodic bending of a particle's trajectory, which arises from the channeling effect, can lead to a new

radiation mechanism, i.e., channeling radiation [23], and to the disappearance of coherent bremsstrahlung, because the theory of this mechanism implies that a particle moves along a straight line at distances of about the radiation formation length.

According to experimental investigations and theoretical calculations, the measured results deviate from those predicted by the coherent bremsstrahlung theory because the particle's straight-line motion approximation is violated. The deviation begins at the crystal axis (or plane) disorientation angles $\psi \leq 5\psi_c$ [24]. When a particle moves with respect to the crystal axis or plane at these angles, its motion is not straight. Hence, the coherent bremsstrahlung mechanism is not fulfilled.

Therefore, the suppression of the coherent bremsstrahlung yield discussed in [11], which is related to the finite sizes of microblocks in mosaic crystals, can manifest itself only if the particle motion trajectory is not bent due to the averaged potential of axes and planes of a crystal. For relativistic electrons, ψ_c is always noticeably greater than the angle ψ, at which the coherent length of photons is close to the microblock sizes in real crystals at the coherent bremsstrahlung spectrum maximum. Hence, the above-discussed effect is masked by the significantly stronger effect of the coherent scattering of particles due to the averaged potential of axes and planes of a crystal. Thus, it is likely that this effect cannot be extracted in the pure form.

The kinematic relations and formulas describing the processes of coherent bremsstrahlung and the coherent generation of electron–positron pairs (CGPs) in oriented crystals resemble each other [22, 25]. Hence, the influence of finite block sizes on the process characteristics [11, 22] can be observed also for the CGPs mechanism. In this case, its coherent length can also be written as $l_{\text{coh}} \approx \delta^{-1}$. However, the minimum transferred longitudinal momentum is defined differently: $\delta = \frac{1}{2\omega}\frac{1}{y(1-y)}$. Here, ω is the photon energy and $y = E_e/\omega$ is the relative energy of any particle of a pair. The distinctive definition of the quantity δ leads to an abrupt decrease in l_{coh}. Thus, even if the photon energy $\omega \sim 10$ GeV, its value does not exceed 10^{-2} μm. On the other hand, manifestation of the suppression effect is not restricted by finite block sizes due to the coherent scattering of particles as in the coherent bremsstrahlung process. Hence, in principle, this effect can appear in the experiment.

It is not ruled out that this effect has already been observed, but has not been interpreted correctly. At the beginning of the 1970s, to create a linearly polarized photon beam with the energy $\omega \sim 10$ GeV via the selective absorption method [26] and to measure the linear polarization of a photon beam with the energy $\omega \sim 16$ GeV [27], mosaic PG crystals with a block mosaicity size of ~1 μm were used [9]. The PG crystals' mosaicity $\sigma_m \geq 3$–4 mrad is substantially greater than the characteristic escape angle of a paired particle with respect to the photon motion direction $\omega^{-1} \sim 0.1$ mrad. In other words, the probability that neighboring blocks are rotated via angle ω^{-1} is close to unity.

PG crystals have a "1 D" reciprocal lattice, i.e., ordered periodicity in one direction. When compared to ordinary 3D crystals, such a structure ensures their undoubted advantage in the creation of polarized beams of high-energy photons and analysis of their polarization [26, 27]. However, PG crystals have not found application in experimental physics to obtain polarized photon beams of high energy because the experimental result of these studies were not coincident with the theoretical calculations according to the CGPs theory [22, 25].

In PG crystals 61 and 31.5 cm thick used as a polarizer and an analyzer in the experiment [27], the measured attenuations of a photon beam with $\omega \approx 16$ GeV turned out to be less than the theoretical values obtained in [25] by ~10%. The authors of the cited study have explained the difference in the results by errors of normalization of the experimental data.

The orientational dependence of the degree of the linear polarization of radiation produced by the selective absorption of high-energy photons in the thick PG crystal, measured with the help of the coherent generation of ρ^0-mesons [26], differed considerably from the theoretical curve [25]. The degree of linear polarization turned out to be less than the calculated value by ~10%. For the reciprocal lattice sites 002 and 004, the values of the coherent effect were less than the calculated values by approximately 40 and 20%, respectively, i.e., differed from the results of measuring the coherent bremsstrahlung spectra of electrons with energies of 870 MeV in the PG crystal of the experiment [29], where good agreement was achieved between the results of measurements with theoretical calculations [22, 25].

The assumption that, for the reciprocal lattice sites 002 and 004, the atomic screening function of the graphite crystal varies by 8 and 12% in comparison with the atomic screening function of a free atom of carbon [28] does not agree with the results of the experiment performed in [29], where the same atomic screening function of a free atom of carbon [28] was used in the calculation, and data on X-ray diffraction in PG crystals [30].

In two performed experiments, the measured coherent effects inherent to the generation of electron–positron pairs in mosaic PG crystals turned out to be less than the theoretically predicted values [22, 25] by approximately 10%. Hence, it can be assumed that the discrepancy between the measured and calculated results is caused by a real physical reason. It is not inconceivable that the true reason is the limitation of block sizes in this crystal. For proving or disproving this hypothesis, it is necessary to perform calculations with allowance for this circumstance and the real conditions of the cited experimental studies, the results of which will be presented later.

CONCLUSIONS

The results of the performed investigations can briefly be summarized as follows.

The $b\alpha$ class of a crystal leads to a cardinal change in the orientation dependence of the diffraction suppression of the fixed-energy bremsstrahlung yield in comparison with measured results [12].

Measurements of the diffraction suppression of the fixed-energy X-ray yield (the X-rays are generated by fast electrons in a crystal) and its comparisons with the suppression measured or calculated for a perfect crystal make it possible to reveal internal blocks rotated at an angle $\Theta \geq \Delta\Theta \sim 10^{-5}$ rad and determine the characteristic longitudinal sizes of microblocks in the crystal under the condition that the recorded suppression is significantly less than the suppression inherent to the $b\alpha$-class crystal with the same characteristic angle of mosaicity.

The technique for estimating the characteristic sizes of microblocks in crystals according to the diffraction suppression of the fixed-energy X-ray yield can be applied not only to accelerators with high energies but also to electron accelerators of moderate energy because the resolution of the crystal-diffraction spectrometer is hardly affected by the electron beam size on the target.

In the practical implementation of the technique in accelerators with a short acceleration cycle, it is reasonable to employ the integral pickup of information from a diffracted radiation detector, which enables us reduce the duration of measurements for one crystallographic plane to 8–10 h.

For relativistic electrons, the effect of axial and planar channeling masks the manifestation of coherent bremsstrahlung due to the finite sizes of blocks in mosaic crystals [11]. Hence, this effect cannot presumably be extracted in the pure form.

In pyrolytic graphite crystals, the finite sizes of microblocks can lead to noncoincidence between the measured and calculated results in the experiments [26, 27]. Confirmation of this hypothesis or elicitation of another reason of noncoincidence makes it possible to return to the use of PG crystals in the formation of photon beams with the high energy ($\omega > 10$ GeV) analysis of their polarization.

ACKNOWLEDGMENTS

We thank the coauthors of [12-14] for participation in the development and implementation of the techniques used in the investigations and their assistance in measurements. This study was supported by the Federal Targeted Program "Scientific and Scientific-Pedagogical Personnel of Innovative Russia" (state contract no. 16.740.11.0147, dated September 2, 2010) and performed under the Program of Internal Grants of Belgorod State University.

REFERENCES

1. V. A. Ryabov, *The Channeling Effect* (Energoatomizdat, Moscow, 1994) [in Russian].
2. S. Datz, B. L. Berman, B. A. Danling, et al., Nucl. Instrum. Methods Phys. Res. B **13**, 19 (1986).
3. R. James, *Optical Principles of the Diffraction of X-Rays* (Cornell Univ., Ithaca, 1965; Inostr. Liter., Moscow, 1950).
4. D. De Salvator, A. Carnera, O. Lytovchenko, et al., in *Proceedings of the Conference on Channeling 2010, 3–8 Oct. 2010, Ferrara, Italy*, p. 74.
5. D. A. Baklanov, I. E. Vnukov, Yu. V. Zhandarmov, et al., Nauch. Vedom. BelGU, Fiz.-Mat., No. 2, 41 (2009).
6. F. Frontera, in *Proceedings of the Conference on Channeling 2010, 3–8 Oct. 2010, Ferrara, Italy*, p. 141.
7. J. R. Santisteban, J. Appl. Crystallogr. **38**, 934 (2005).
8. D. A. Baklanov, I. E. Vnukov, Yu. V. Zhandarmov, and R. A. Shatokhin, J. Surf. Invest. **4**, 295 (2010).
9. M. Ohler, J. Baruchel, A. W. Moore, Ph. Galez, and A. Freund, Nucl. Instrum. Methods Phys. Res. B **129**, 257 (1997).
10. S. S. Gorelik, Yu. A. Skakov, and L. N. Rastorguev, *X-Ray Diffraction and Electron-Optical Analysis* (MISIS, Moscow, 2002) [in Russian].
11. D. A. Baklanov, I. E. Vnukov, Yu. V. Zhandarmov, et al., J. Surf. Invest. **5**, 310 (2011).
12. A. N. Aleinik, A. N. Baldin, E. A. Bogomazova, et al., JETP Lett. **80**, 393 (2004).
13. I. E. Vnukov, B. N. Kalinin, A. A. Kir'yakov, et al., Izv. Vyssh. Uchebn. Zaved., Fiz. **44** (3), 71 (2001).
14. A. N. Baldin, I. E. Vnukov, B. N. Kalinin, and E. A. Karataeva, Poverkhnost', No. 4, 72 (2006).
15. D. A. Baklanov, I. E. Vnukov, Yu. V. Zhandarmov, et al., J. Surf. Invest. **5**, 317 (2011).
16. D. A. Baklanov, T. G. Duong, S. A. Laktionova, et al., Nuovo Cimento. doi:10.1393/ncc/i2011-10933-7.
17. Z. G. Pinsker, *X-ray Crystal Optics* (Moscow, Nauka, 1982) [in Russian].
18. V. I. Shvedunov, A. N. Ermakov, A. I. Karev, et al., in *Proceedings of the 2001 Particle Accelerator Conference, Chicago* (2001), p. 2596.
19. A. V. Shchagin, V. I. Pristupa, and N. A. Khizhnyak, Phys. Lett. A **148**, 485 (1990).
20. D. A. Baklanov, I. E. Vnukov, V. K. Grishin, et al., J. Surf. Invest. **4**, 203 (2010).
21. B. N. Kalinin, G. A. Naumenko, A. P. Potylitsin, et al., Nucl. Instrum. Methods Phys. Res. B **145**, 209 (1998).
22. M. L. Ter-Mikaelyan, *The Influence of the Medium on High-Energy Electromagnetic Processes* (Izd-vo AN ARM SSR, Yerevan, 1969) [in Russian].
23. M. A. Kumakhov, *Radiation of Channeled Electrons in Crystals* (Energoatomizdat, Moscow, 1986) [in Russian].
24. L. E. Gendel'shtein and E. V. Pegushin, Sov. Tech. Phys. **29**, 21 (1984).
25. G. Diambrini, Rev. Mod. Phys. **40**, 611 (1968).
26. C. Berger, G. McClellan, N. Mistry, et al., Phys. Rev. Lett. **25**, 1366 (1970).
27. R. L. Eisele, D. J. Sherden, R. H. Siemann, et al., Nucl. Instrum. Methods Phys. Res. **113**, 489 (1973).
28. D. T. Cromer and J. T. Waber, Acta Crystallogr. **8**, 104 (1965).
29. I. E. Vnukov, Izv. Vyssh. Uchebn. Zaved., Fiz. **45** (9), 66 (2002).
30. M. Chabot, P. Nicolai, K. Wohrer, et al., Nucl. Instrum. Methods Phys. Res. B **61**, 377 (1991).